

Article

Design of an Antipodal Vivaldi Antenna Using RSIW Technology

Priscilla Kadja P. de M. Carneiro¹ , Maraiza Prescila dos Santos² , Alfredo Gomes Neto³ ,
Alexandre Jean R. Serres¹ , Adolfo F. Herbster¹ 

¹Federal University of Campina Grande, UFCG, Paraíba, Brazil, priscilla.melo@ee.ufcg.edu.br,
alexandreserres@dee.ufcg.edu.br, adolfofh@dee.ufcg.edu.br

²Federal Institute of Paraíba, IFPB, Paraíba, Brazil, maraiza.santos@ifpb.edu.br

³Group of Telecommunications and Applied Electromagnetism, GTEMA, Federal Institute of Paraíba, IFPB,
Paraíba, Brazil, alfredogomes@ifpb.edu.br

Abstract— This paper proposes a methodology for developing antipodal Vivaldi antennas using RSIW (Ridge Substrate Integrated Waveguide) technology for a specific cut-off frequency. The technique employs metallic-vias and metalized cylindrical posts of reduced sizes inserted in the dielectric substrate. The simulations were performed using the ANSYS® Electronics Desktop software. The antenna RSIW is designed for a resonant frequency of 4 GHz and was fabricated on FR4 ($\epsilon_r=4.4$ and $\tan\delta=0.02$). The structure is compared to an antipodal Vivaldi antenna (AVA) fed by a SIW. The structure proposed had an increase in bandwidth of 4.09 GHz and an increase in gain of 1.41 dBi.

Index Terms— Antipodal Vivaldi Antenna, Bandwidth Enhancement, Directivity Improvement, Ridged Substrate Integrated Waveguide.

I. INTRODUCTION

The advancement in wireless communication networks requires antennas with reduced size, multiband operation, low cost, and acceptable gain [1]. In 2001, a new technology called Substrate Integrated Waveguide (SIW) was proposed [2]. In this context, the SIW technology is attractive for components that operate in the microwave and millimeter wave ranges. The SIW combines the advantages of planar and non-planar technologies, utilizes the printed circuit board (PCB), and enables a compact and lightweight design [3]. However, the technology presents dielectric losses that increase at high frequencies. In this context, a topology of the SIC (Substrate Integrated Circuits) called ridge substrate integrated waveguide (RSIW) is presented. It is composed of metallic-vias and metalized cylindrical posts of variable heights inserted in the dielectric substrate [4], [5].

The reference antenna for this project is the antipodal Vivaldi Antenna (AVA). AVA has a planar structure, low profile, ultra-wide bandwidth, directive radiation patterns, high efficiency, linear polarization, small dimensions, and printed circuit compatibility, allowing easy integration with other wireless components [6], [7].

Different methods are presented in [3] to enhance the performance of the antipodal Vivaldi antenna and can be used in conjunction with the aforementioned techniques. Modifying the shape of the radiating element using slots improves antenna characteristics such as bandwidth, greater directivity, and gain. In addition to minimizing the lower cutoff frequency, reducing sidelobe levels, and increasing the main lobe level [8], [9]. An Antipodal Vivaldi antenna with rectangular slots and using SIW technology was proposed in [9], with wide bandwidth covering almost the entire D band from 110 to

163 GHz, with a gain of 9.02 dBi at 137.2 GHz. In [10], an antipodal Vivaldi antenna with elliptical slots is presented and the antenna gain is increased by about 1 to 2.6 dBi within the frequency range of 7 to 25 GHz.

In this paper, a methodology for the development of antipodal Vivaldi antennas using RSIW technology for a specific cut-off frequency is presented. The insertion of ridges allows for bandwidth enhancement due reduction to the cut-off frequency and, consequently, enabling miniaturization. Finally, the insertion of the slots promotes an increase in gain, bandwidth, and a decrease in half-power beam width. The new structure is compared to the one powered by a SIW designed for a cut-off frequency close to 4 GHz, which had an increase in bandwidth of 4.09 GHz, a gain increase of 1.41 in gain, and a 10° decrease in half-power beamwidth. Simulations were performed in ANSYS® Electronics Desktop and compared with measurements.

This paper is organized as follows: Section II presents the project methodology. Section III presents the design procedures for the new structure. The results are presented in Section IV. Finally, conclusions are drawn in Section V.

II. METHODOLOGY

This section presents the methodology used for the design of Antipodals Vivaldi antennas with RSIW technology using slots. The antenna chosen as a reference for this project is made up of a microstrip transmission line power system and an exponential slot line radiator (ESLR). Fig. 1 illustrates the antenna indicating the five stages of the project.

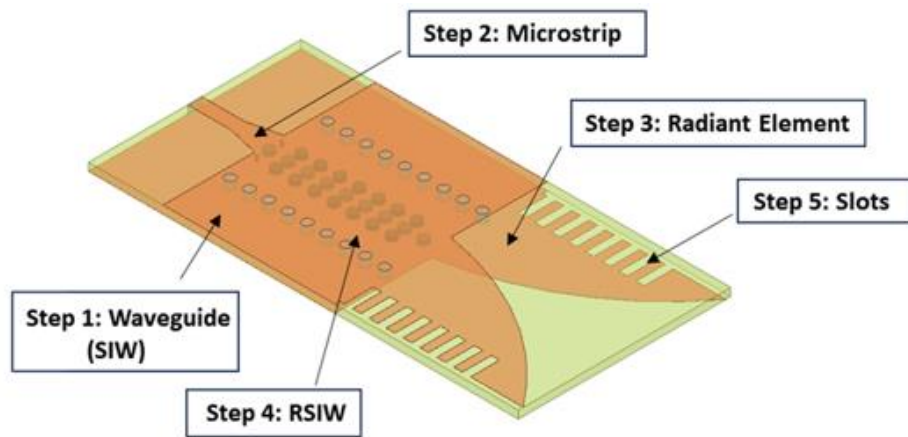


Fig. 1: Development stages of the proposed antenna.

A. Step 1: Waveguide (SIW)

The design parameters of the SIW structure are shown in Fig. 2. The first step was to calculate the width between the waveguide vias ($W2$), given by (1) for the desired cut-off frequency, $f_c = 4$ GHz. In this way, the width between the vias (W_{eff}) is calculated by (2) [11].

$$W2 = \frac{d^2}{2f_c \sqrt{\epsilon_r}} \quad (1)$$

where, ϵ_r is the relative permittivity and d is the diameter of the via.

$$W_{eff} = W + d \quad (2)$$

Then, the length value of the SIW (L_{eff}) is defined by (3) [12].

$$L_{eff} = -1.08 \frac{d^2}{p} + 0.1 \frac{d^2}{1}. \quad (3)$$

For the SIW design, the vias have diameters (d) of 2 mm, periodically spaced by a distance (p) of 4 mm, respecting the rules presented in [12].

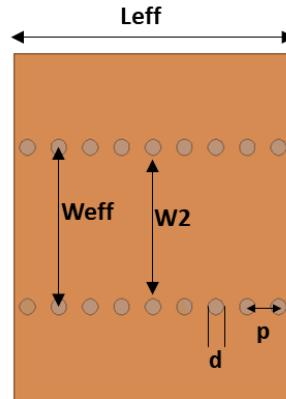


Fig. 2: SIW structure parameters.

B. Step 2: Microstrip and SIW Transition

The antenna is fed by a microstrip line of 50Ω , and its dimensions were calculated by (4) [13]:

$$\frac{W_f}{h} = \frac{2}{\pi} \left\{ B - 1 - \ln(2B - 1) + \frac{\epsilon_r - 1}{2\epsilon_r} \left[\ln(B - 1) + 0.39 - \frac{0.61}{\epsilon_r} \right] \right\} \quad (4)$$

where, h is the height of the substrate and B is given by (5):

$$B = \frac{377\pi}{2Z_0\sqrt{\epsilon_r}} \quad (5)$$

The length of the microstrip line (L_f) is given by (6) [14].

$$L_f = \lambda/2 \quad (6)$$

The tapers were designed with the width of the input port fixed to the width of the microstrip transmission line. For taper length (L_1), multiples of $\lambda/4$ should be used to minimize return loss and the width of the exit port (W_1) is calculated by (7) [14]. The (L_1) value was initially $\lambda/4$, but for a better impedance matching the value used was 6.4 mm. The integration between the microstrip line and the SIW technology is shown in Fig. 3.

$$W_1 = W_f + 0.1547 \times W_{eff} \quad (7)$$

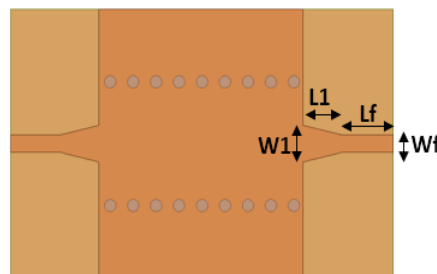


Fig. 3: Integration between the microstrip line and the SIW technology.

C. Step 3: Radiant Element

The value for the length (L_s) is defined in [15], its value must be at least $\lambda_0/2$. Fig. 4 illustrates the AVA SIW.

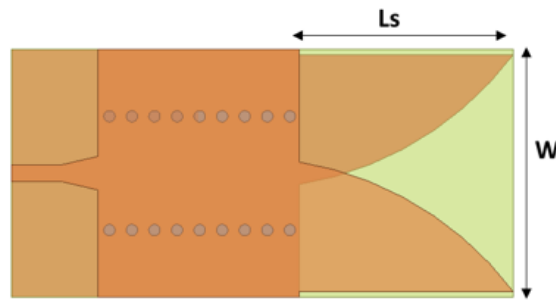


Fig. 4: AVA SIW.

D. Step 4 RSIW

The next step is the insertion of RSIW technology. Fig. 5 illustrates the AVA RSIW. The ridge has only one end connected to the ground plane and has spacing with length g , which introduces a capacitive effect on the waveguide [16].

The ridge is composed of three lines of metalized cylindrical posts inserted into the substrate with a height of 0.8 mm. The diameter and space between the ridge posts are the same as those used in the SIW metallic-vias. The SIW is composed of nine metallic-vias on each side and the central row of ridges consists of nine metalized cylindrical posts inserted in the dielectric. To avoid the loss of electromagnetic energy, two ridges with minor radius are inserted at the transition between the taper and the SIW, as suggested by [17]. The cut-off frequency of an RSIW waveguide can be changed by adjusting the width and height of the ridge without changing the outer dimensions of the waveguide [16]. The value of $P2$ is half the width of the ridge.

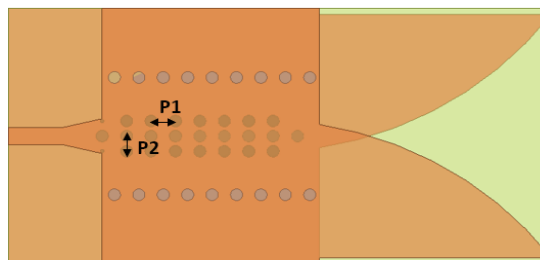


Fig. 5: AVA RSIW.

E. Step 5: SLOTS

The incorporation of slots does not affect the final dimensions of the antenna compared to the reference antenna, nor does it impede the construction process [15], [18]. Fig. 6 illustrates the rectangular slots employed in the AVA RSIW.

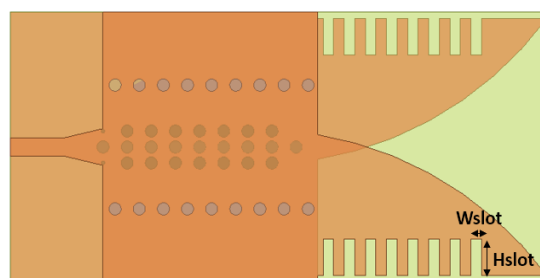


Fig. 6: AVA RSIW rectangular slots.

This technique aims to improve the bandwidth, decrease the lowest cutoff frequency, reduce the side lobe levels, and increase the main lobe level. The slot length value (W_{slot}) utilized in this project underwent numerical optimization, approximating $\lambda/2$.

III. AVA DESIGN

The antenna design was simulated on FR4 ($\epsilon_r = 4.4$ and $\tan\delta = 0.02$). The metallic vias were inserted on both sides to emulate the waveguide effect, and metallic posts ($h = 0.8$ mm) were inserted on the center of the substrate for the ridge effect.

The antenna proposed in this paper exhibits a cut-off frequency close to 4 GHz. Fig. 7 shows the antenna AVA RSIW rectangular slots. Table I shows the dimensions of the AVA RSIW rectangular slots.

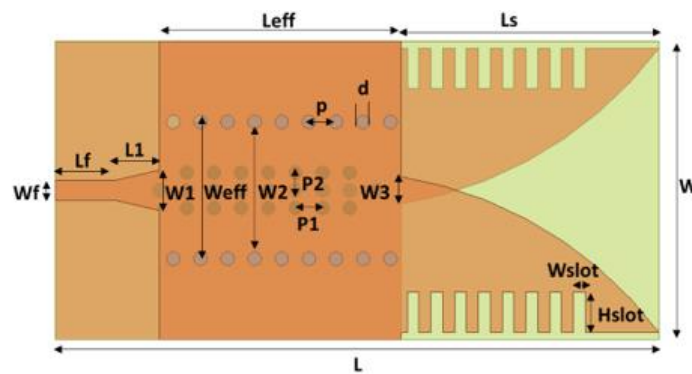


Fig. 7: Parameters of the proposed AVA RSIW.

TABLE I. PARAMETERS OF THE AVA RSIW.

Parameter	Value (mm)
Wf	2.92
W	42
L	89
L1	6.4
Lf	10.27
Ls	37.9
Weff	19.8
Leff	35.6
W1	6
W2	17.8
W3	4
D	2
P	4
P1	4
P2	2.6
Wslot	1.7
Hslot	8

IV. NUMERICAL AND EXPERIMENTAL RESULTS

In this section, the numerical results for the designed antennas are presented. As an example, it is presented the design for an antenna using RSIW technology, with a cut-off frequency of 4 GHz, following the steps given in Fig. 1. The simulations were performed using the High Frequency Structure Simulator (HFSS) software from ANSYS Electronics Desktop.

The antenna presented in this paper was fabricated using a PCB process. The holes were made in the substrate using an LPKF (Protomat S43) milling machine. Next, the geometry is printed on a sticker and affixed to the surface of the structure. Subsequently, the metallic surface that is not part of the antenna is removed through a corrosion process using iron perchloride.

The metallic-vias were metalized by inserting metal screws with the same diameter as the holes and an SMA connector was used in the antenna input. In the antenna with the SIW, a plate of 1.6 mm thickness was used, with the RSIW two plates with 0.8 mm thickness each were used, with the cylindrical posts made in one of the plates. The cylindrical posts were inserted in the dielectric substrate with a height of 0.8 mm and were filled with a solder paste. Fig. 8 (a) illustrates the top view and Fig. 8 (b) bottom view fabricated AVA RSIW rectangular slots.

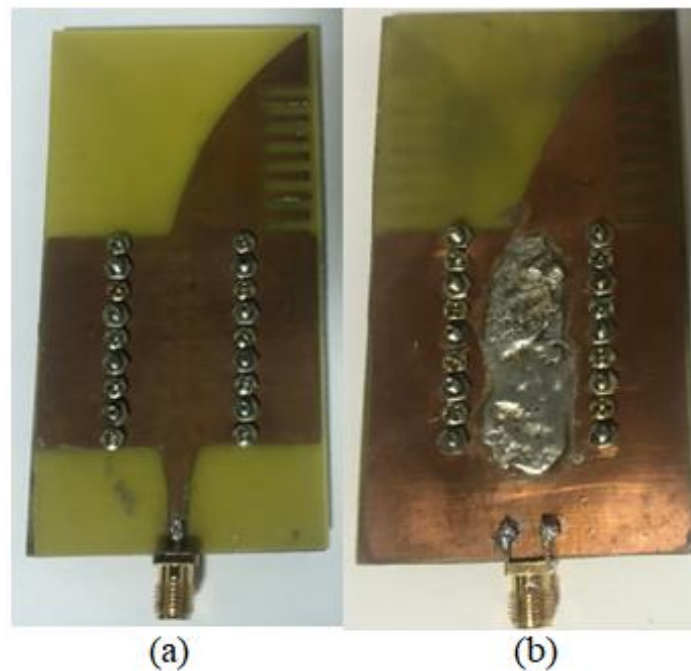


Fig. 8: AVA RSIW rectangular slots fabricated (a) Top view (b) Bottom view.

The measurements were carried out using a network analyzer (Agilent - ENA E5071C), the proposed antenna as a transmitter (Tx), and a double ridge guide (A. H. Systems - model SAS571) as a receiving antenna (Rx). The distance between the transmitting and receiving antennas is 1.3 m and the measurement was performed every 5 degrees. The measurement setup is shown in Fig. 9.

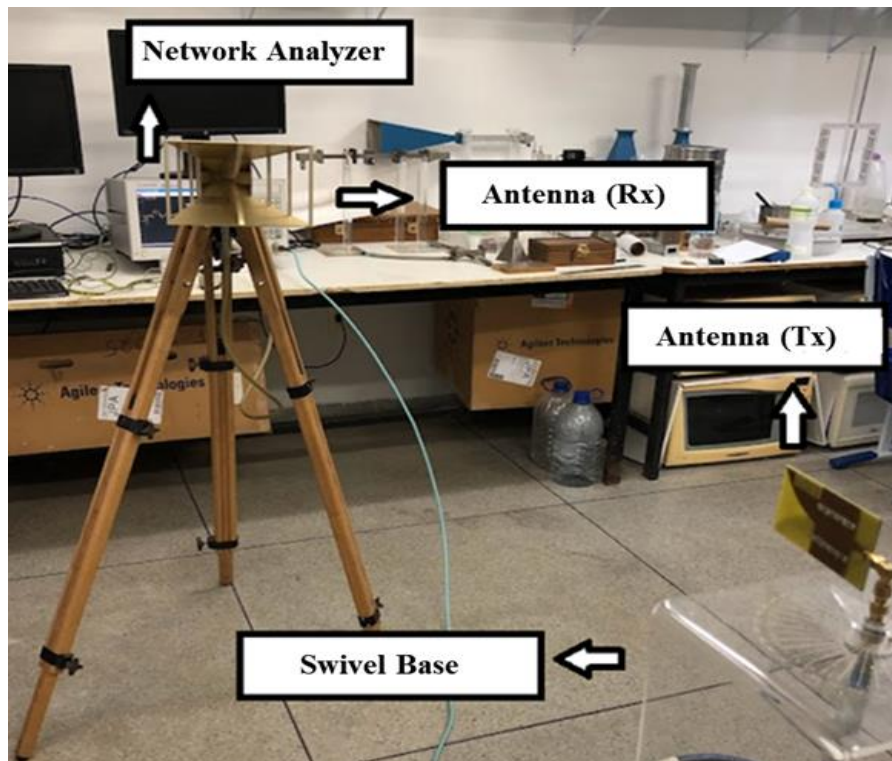


Fig. 9: Measurement setup.

In the first step, the dimensions of the SIW waveguide were defined for the desired cut-off frequency. The values were calculated based on the equations presented in the methodology. On each side of the structure, there is a Lumped Port type. The values used are presented in Table I. Fig. 10 (a) illustrates the geometry and Fig. 10 (b) presents the simulated reflection coefficient (S11) and transmission coefficient (S21) of the equivalent waveguide. It is possible to observe that the cut-off frequency of the structure at -10 dB is 4 GHz.

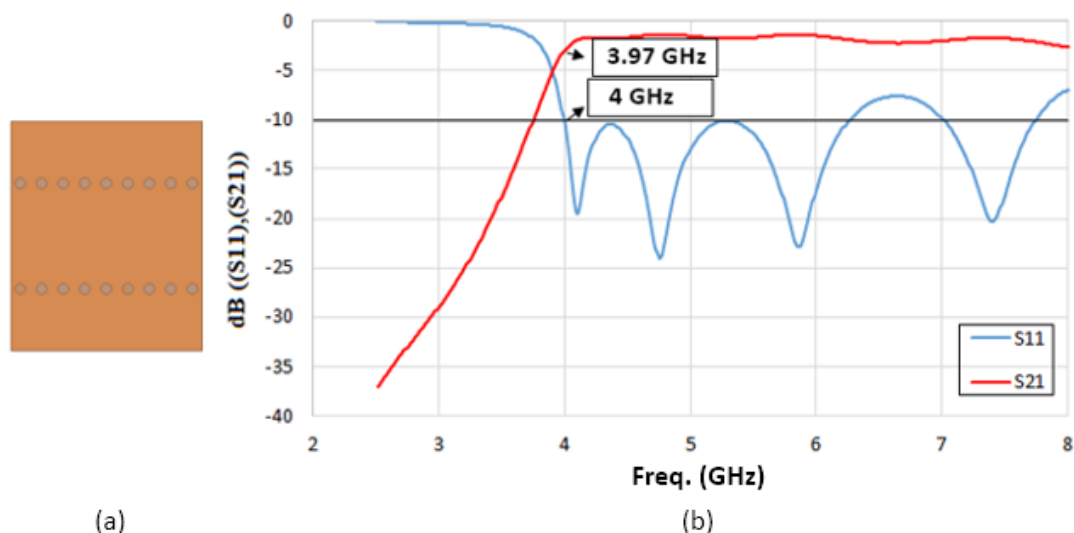


Fig. 10. Equivalent waveguide (a) Geometry (b) S11 and S21.

The second step is the insertion of the microstrip line with a characteristic impedance of 50 Ω . Fig. 11 (a) illustrates the geometry and Fig. 11 (b) presents the simulation of S11 and S21 of the integration

between the microstrip line and the SIW technology. The transition line and the microstrip feed line were integrated into the SIW structure with good impedance matching and a cut-off frequency at -10 dB of 4.04 GHz, very close to the frequency obtained in the first step of this methodology. Additionally, a reduction in the S11 values can be observed compared to structures with only SIW.

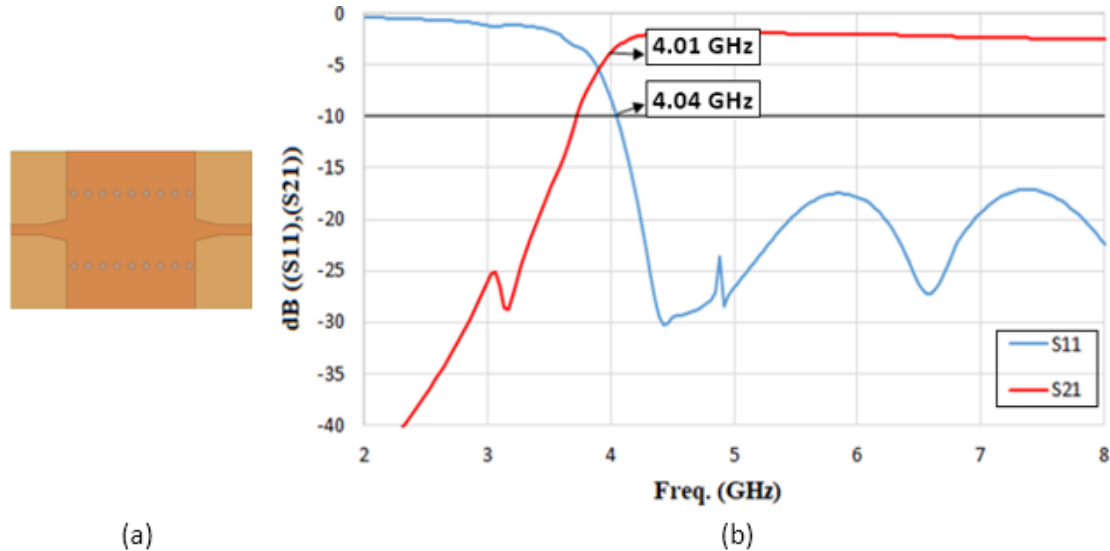


Fig. 11. Integration between the microstrip line and the SIW technology. (a) Geometry (b) S11 and S21.

The third stage consists of inserting the radiating element of the SIW antenna. Fig. 12 (a) illustrates the geometry of the AVA SIW and the result of the reflection parameters is shown in Fig. 12 (b). It is possible to observe the S11 below -10 dB from the cut-off frequency f_c of 4.15 GHz to the frequency of 9.46 GHz, which represents a bandwidth of 5.31 GHz.

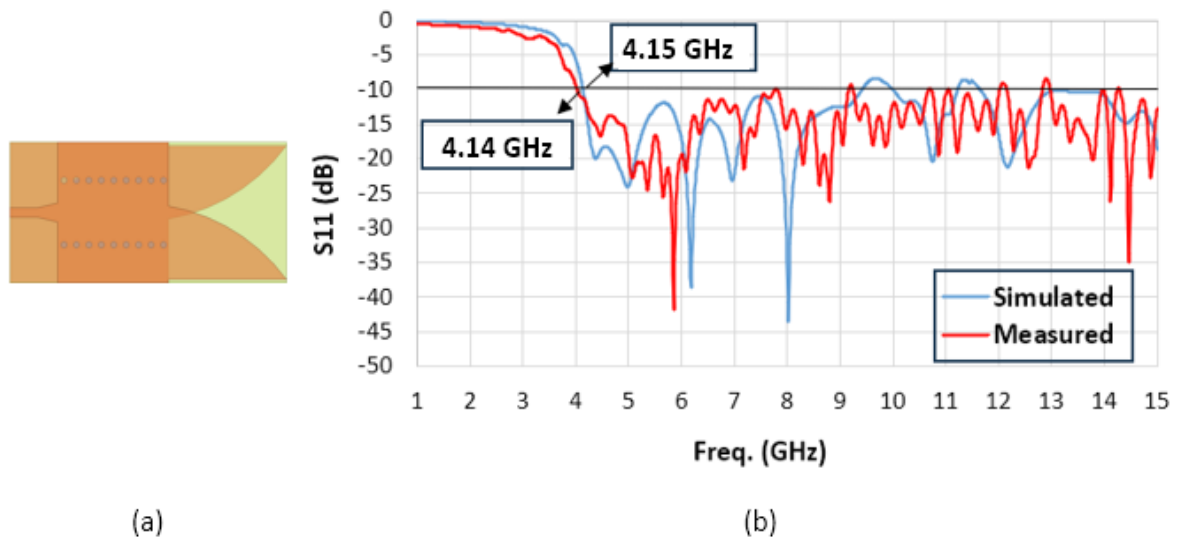


Fig. 12: AVA SIW (a) Geometry (b) Parameter S11.

Fig. 13 (a) illustrates the geometry 3D and Fig. 13 (b), (c) and (d) presents the 2D radiation patterns and half-power beamwidth (HPBW) of the AVA SIW at three different frequencies. Diagrams are simulated with the lower frequency (4.15 GHz), the central frequency (6 GHz), and the upper frequency (9.46 GHz). AVA SIW presented a gain of 5.29 dBi and a beamwidth of 68° at the center frequency.

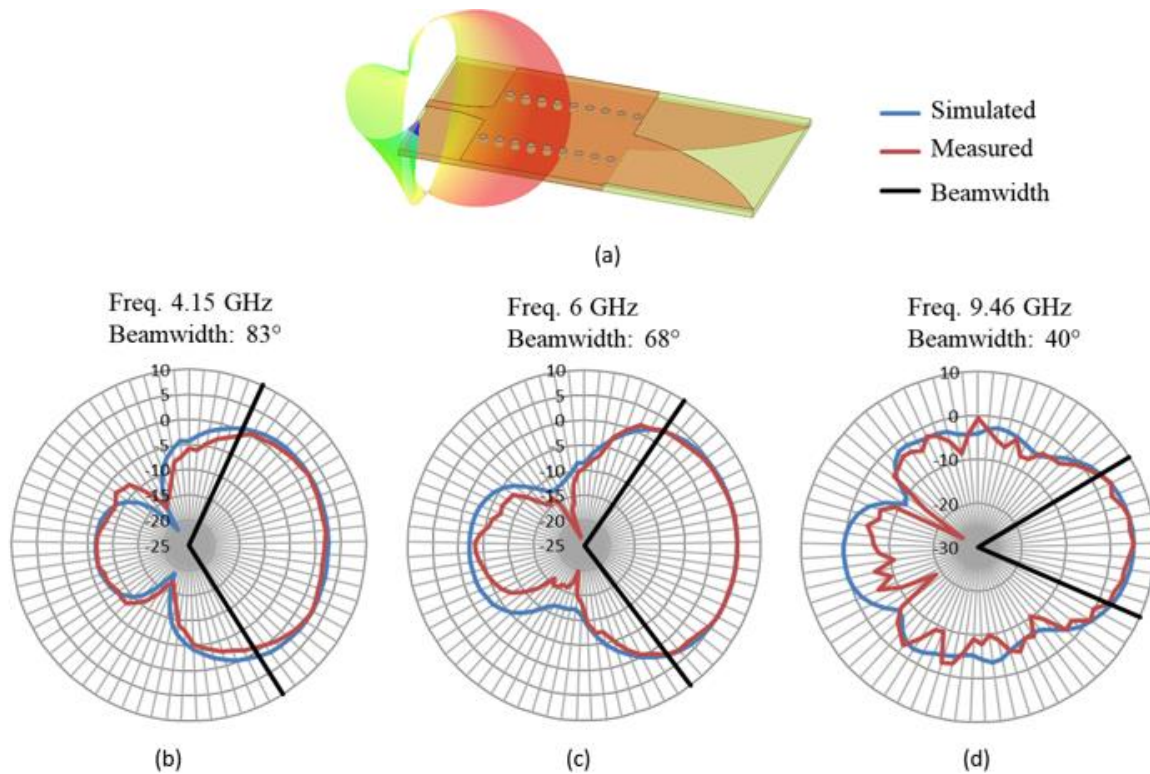


Fig. 13. AVA SIW 3D and 2D radiation patterns and beamwidth, with PHI = 90°: a) 3D, b) $f_c = 4.15$, c) $f_c = 6$ GHz and d) $f_c = 9.46$ GHz.

The next step is the insertion of technology RSIW. Fig 14 (a) illustrates the geometry and the simulated and measured reflection coefficient of the AVA RSIW is given in Fig. 14 (b).

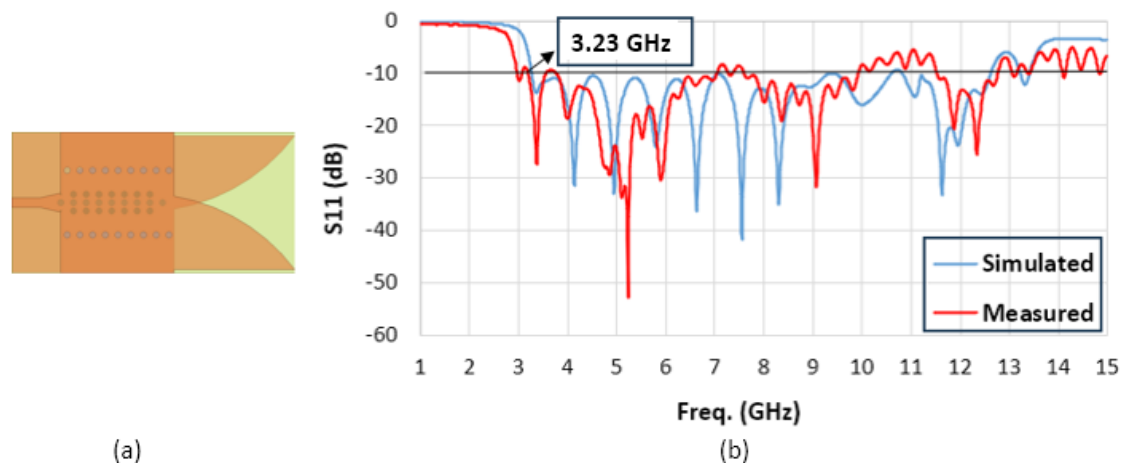


Fig. 14: S11 AVA RSIW (a) Geometry (b) Parameter S11.

The cut-off frequency AVA SIW is 4.15 GHz (value close to the desired frequency) with a bandwidth of 5.31 GHz. The cut-off frequency of the AVA RSIW is 3.23 GHz, which is 0.92 GHz lower than that of the AVA SIW, boasting a bandwidth of 7.37 GHz and marking a significant 2.06 GHz increase. This reduction in the cut-off frequency could potentially contribute to a more compact structure.

Fig. 15 (a) illustrates the geometry 3D and Fig. 15 (b), (c) and (d) presents the 2D radiation patterns half-power beamwidth of the AVA RSIW at three different frequencies. Diagrams are simulated with

the lower frequency (3.23 GHz), the central frequency (6 GHz), and the upper frequency (10.6 GHz).

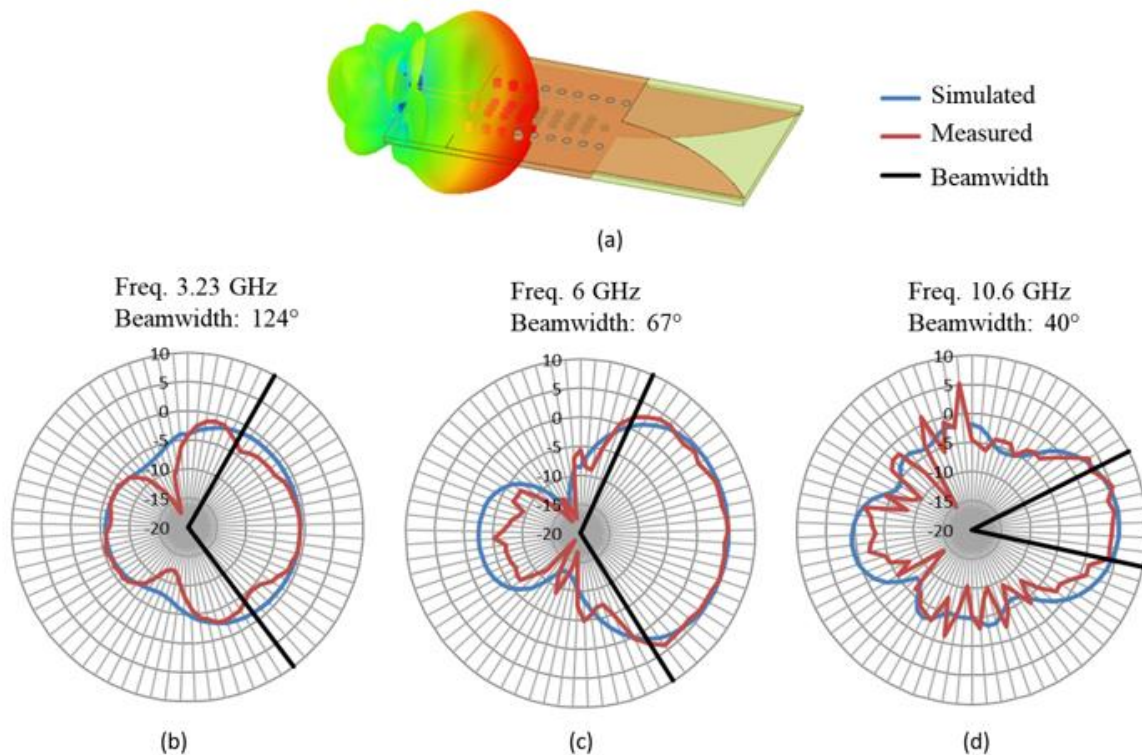


Fig. 15: AVA RSIW 3D and 2D radiation patterns and beamwidth, with PHI = 90°: a) 3D, b) $f_c = 3.23$, c) $f_c = 6$ GHz and d) $f_c = 10.6$ GHz.

The AVA RSIW, in addition to increasing the antenna bandwidth, showed an increase in the maximum gain at the 6 GHz frequency from 5.29 dBi to 5.37 dBi.

The fifth stage consists of introducing the slots. Fig. 16 (a) illustrates the geometry and Fig. 16 (b) the reflection coefficients of the AVA RSIW rectangular slot antennas. The cut-off frequency of the AVA RSIW rectangular slot is 3.44 GHz, 0.7 GHz lower than the AVA SIW and an improved bandwidth of 3.81 GHz is obtained.

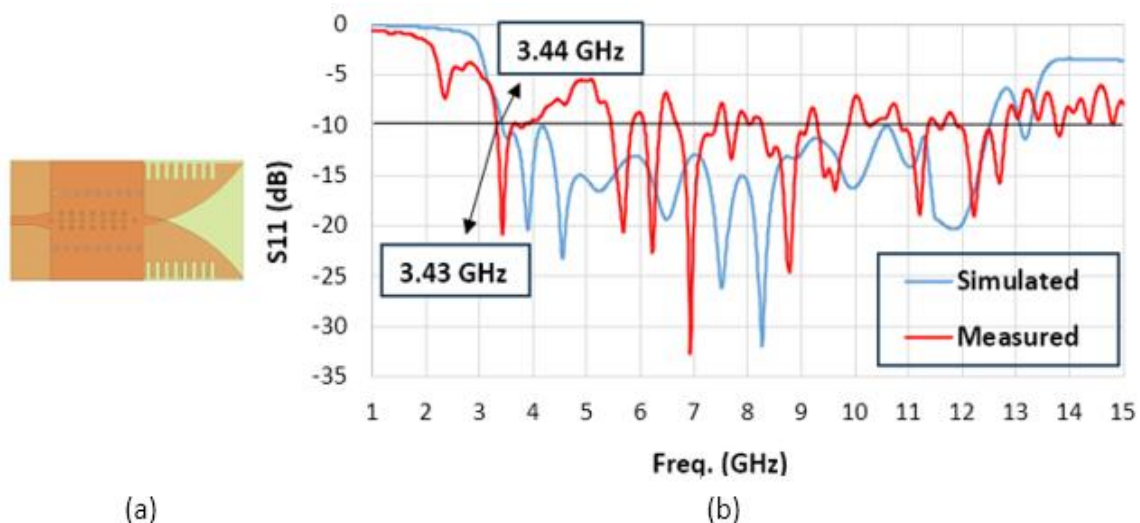


Fig. 16: AVA RSIW rectangular slot (a) Geometry (b) Parameter S11.

In Fig. 17 (a) illustrates the geometry 3D and Fig. 17 (b), (c) and (d) presents the 2D radiation patterns and half-power beamwidth. The gain of the AVA RSIW with rectangular slots was 6.57 dBi at the center frequency and a beamwidth of 63° . In the results could be noticed the expected increase in gain and the decrease in half-power beam width. Furthermore, directivity also increases with decreasing side lobe level (SLL).

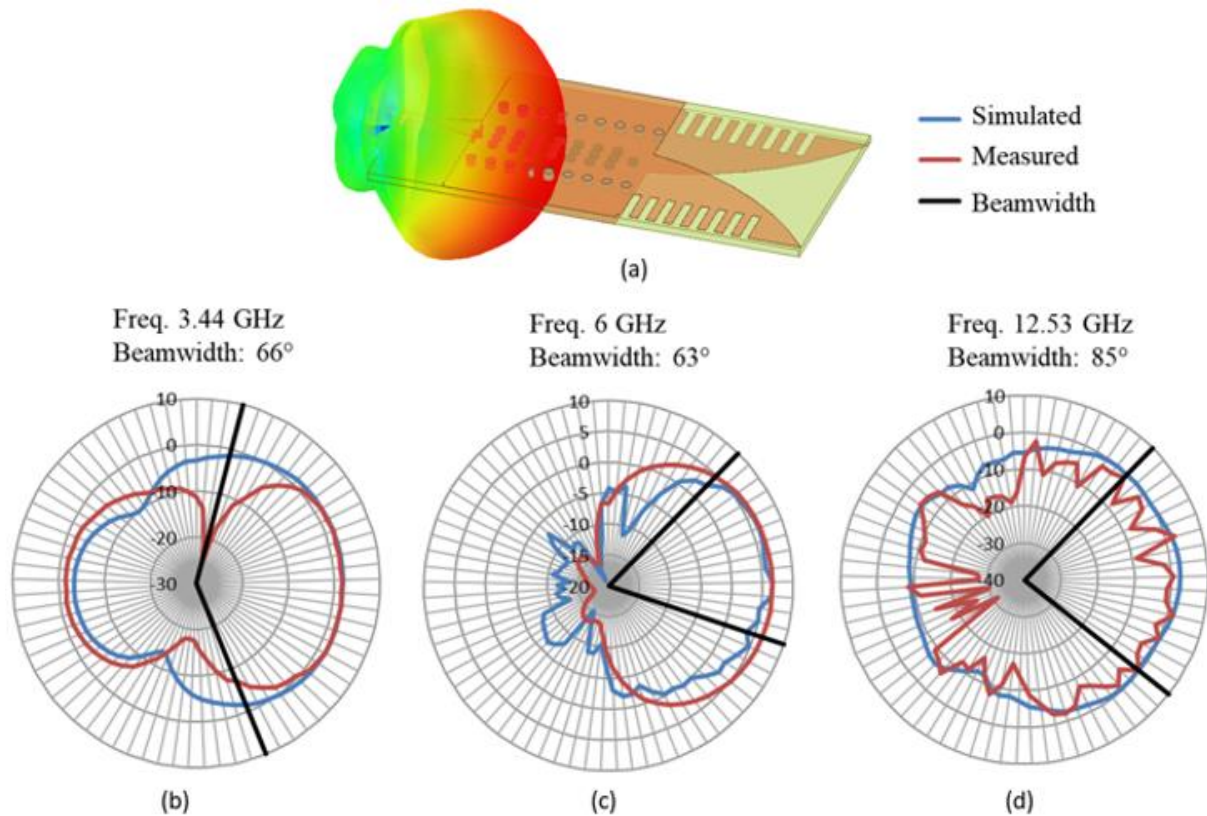


Fig. 17: AVA RSIW rectangular slots 3D and 2D radiation patterns and beamwidth, with $\text{PHI} = 90^\circ$: a) 3D, b) $f_c = 3.44$ GHz, c) $f_c = 6$ GHz and d) $f_c = 12.53$ GHz.

The application of this technique to the SIW antenna showed an increase in bandwidth, gain, and directivity. Then, another slot format was tested. The ellipse shaped slot was presented in [9] in order to increase the antenna gain. The size ($H_{\text{slot}} = 8$ mm) and the distance ($W_{\text{slot}} = 1.7$ mm) between the slots are the same as those used for rectangular slots.

The geometry of the AVA RSIW elliptical slots is illustrated in Fig. 18 (a) and the simulated and measured reflection coefficient is given in Fig. 18 (b). The cut-off frequency of the AVA elliptical slots is 0.22 GHz lower than the AVA rectangular slots, and an improved bandwidth of 0.32 GHz is obtained. The AVA RSIW elliptical slot compared to the AVA SIW features a cut-off frequency reduction of 0.93 GHz, a 4.09 dBi increase in gain, and a 10° reduction in half-power beamwidth. By reducing the cutting frequency, the structure achieves smaller electrical dimensions. As a result, it becomes feasible to construct a smaller-sized structure while maintaining the same cut-off frequency.

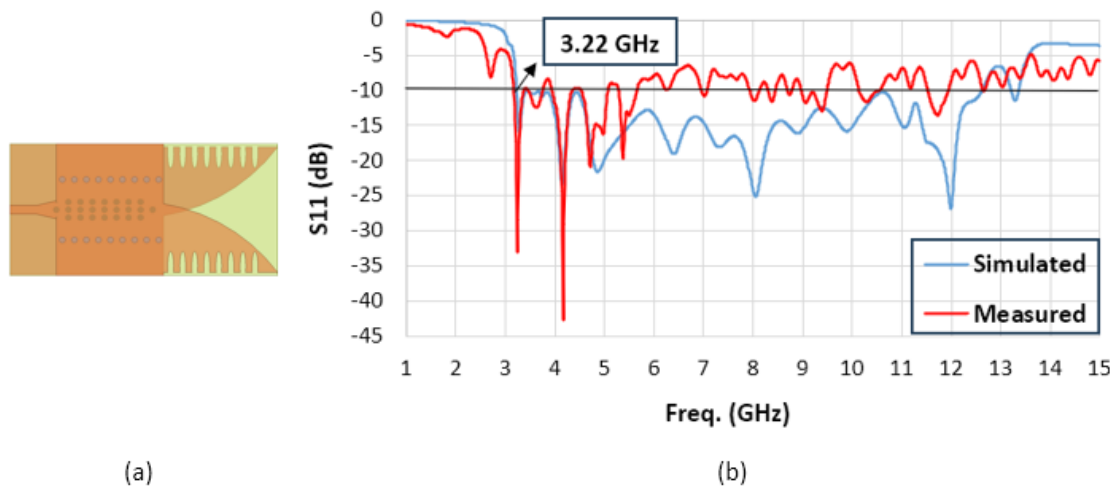


Fig.18: AVA RSIW elliptical slots (a) Geometry (b) Parameter S11.

Fig. 19 (a) illustrates the geometry 3D and Fig. 19 (b), (c) and (d) presents the 2D radiation patterns and the beamwidth of the AVA RSIW elliptical slots. Diagrams are simulated with the lower frequency (3.22 GHz), the central frequency (6 GHz), and the upper frequency (12.62 GHz). The AVA RSIW elliptical slots showed a gain of 6.7 dBi at a frequency of 6 GHz and a beam width of 58°. This antenna demonstrated superior performance compared to the AVA RSIW rectangular slots configuration.

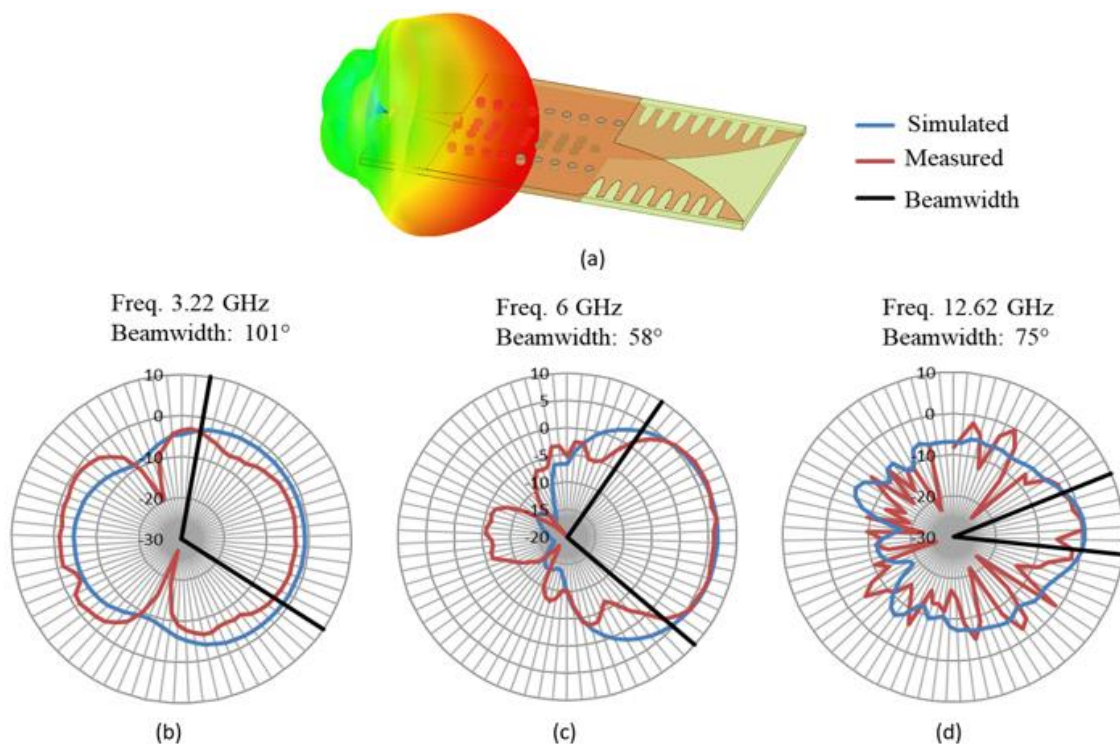


Fig. 19: AVA RSIW elliptical 3D and 2D radiation patterns and beamwidth, with $\text{PHI} = 90^\circ$: a) 3D, b) $f_c = 3.22$ GHz, c) $f_c = 6$ GHz and d) $f_c = 12.62$ GHz.

The result of the AVA RSIW rectangular slots and AVA RSIW elliptical slots measured are starting with the same cut-off frequency as the result of the simulated antennas. The AVA RSIW rectangular slots have some degradations, like the first peak above -10 dB between the 4 and 5 GHz frequencies and others afterwards, presented in Fig. 16 (b). In the graph of parameter S11 of the AVA RSIW

elliptical slots, presented in Fig. 18 (b), there were peaks above -10 dB after the 5 GHz frequency. There was also a reduction in the return loss (S11) in the measured antenna. The degradation observed in the S11 parameters across certain frequency bands can be attributed to factors encountered during the antenna fabrication process, particularly since it was conducted using a homemade method. Additionally, discrepancies may have arisen during the antenna measurement phase. Table II illustrates a comparison of the irradiation parameters of the designed antennas.

TABLE II: RADIATION PARAMETERS OF SIW, RSIW, RSIW RECTANGULAR SLOT AND AVA RSIW ELLIPTIC SLOT.

ANTENNA	BW (GHz)	HPBW (f_0)	GAIN (dBi)
SIW	5.31	68°	5.29
RSIW	7.37	67°	5.37
RECTANGULAR	9.08	63°	6.57
ELLIPTICAL	9.4	58°	6.7

V. CONCLUSIONS

A Vivaldi Antipodal antenna with SIW technology is proposed, designed using a low-cost, single-layer FR4 substrate with a thickness of 1.6 mm. There is a good correlation between the model and the prototypes. Two techniques were then introduced to improve the irradiation properties. The first technique is the insertion of the RSIW. These structures add SIW characteristics, provide an increase in operational bandwidth, and reduce the cutoff frequency. Furthermore, they are compact structures. The second technique is the addition of slits to the edge of the antenna's radiating element to improve the antenna's characteristics. This technique aims to improve bandwidth, decrease the lower cutoff frequency, reduce sidelobe levels, and increase the main lobe level.

The insertion of rows of ridges demonstrated advantages, such as increased bandwidth and, consequently lower frequency that can lead to a more compact structure, and increased gain. After inserting slots, it is possible to observe that in the antenna with RSIW there was an improvement in the results of the antenna, including the gain, which had an increase of 1.41 dBi and a reduction of 10° in the half-power beamwidth, without increasing the degree of complexity of antenna construction.

ACKNOWLEDGMENT

The authors thank the support from the Federal University of Campina Grande Graduate Coordination in Electrical Engineering (COPELE/UFCG), the Group of Telecommunications and Applied Electromagnetism of the Federal Institute of Education, Science and Technology of Paraíba (GTEMA/IFPB) and Coordination of Superior Level Staff Improvement (CAPES).

REFERENCES

- [1] Hanumanthappa and R. Immaculate, "SIW based mono-pole antenna for WLAN and WIMAX applications," *2nd IEEE International Conference on Recent Trends in Electronics, Information & Communication Technology (RTEICT)*, 2017. DOI: 10.1109/RTEICT.2017.8256751
- [2] D. Deslandes and K. Wu, "Integrated microstrip and rectangular waveguide in planar form," *IEEE Microwave and Wireless Components Letters*, vol. 11, no. 2, pp. 68 - 70, 2001. DOI: 10.1109/7260.914305

- [3] A.S. Dixit and S. Kumar, "A Survey of Performance Enhancement Techniques of Antipodal Vivaldi Antenna," *IEEE Access*, vol. 8, pp. 45774 - 45796, 2020. DOI: 10.1109/ACCESS.2020.2977167
- [4] M. P. Santos, R. C. S. Freire, H. M. Baundrand, G. K. F. Serres and A. J. R. Serres, "Compact Band-pass Filter with RSIW Cavity," *13th European Conference on Antennas and Propagation (EuCAP)*, 2019.
- [5] M. Bozzi, S. A. Winkler and K. Wu, "Novel Compact and Broadband Interconnects based on Ridge Substrate Integrated Waveguide," *IEEE MTT-S International Microwave Symposium Digest*, 2009. DOI: 10.1109/MWSYM.2009.5165647
- [6] L. Zhou, M. Tang and J. Mao, "3-D Printed Vivaldi Antenna Fed by SIW Slot for Millimeter-Wave Applications," *International Conference on Microwave and Millimeter Wave Technology (ICMMT)*, 2021. DOI: 10.1109/ICMMT52847.2021.9617844
- [7] G. Kumar and K. Ray, in *Broadband Microstrip Antennas.*, Artech, 2002.
- [8] M. A. Ashraf, I. Memon and S. A. Alshebeili, "Design and analysis of broadband antipodal Vivaldi antenna for radio over fiber systems," *Microwave and Optical Technology Letters*, vol. 59, no. 6, 2017. DOI: <https://doi.org/10.1002/mop.30560>
- [9] L. N. V. Kumar and M. Swaminathan, "Ultra-Wide Bandwidth Substrate Integrated Waveguide Fed Vivaldi Antenna in D-Band Using Glass Interposer," *IEEE Radio and Wireless Symposium (RWS)*, 2023. DOI: 10.1109/RWS55624.2023.10046328
- [10] Z. Yin, X. Yang and T. Lou, "A High Gain UWB Vivaldi Antenna Loaded with Elliptical Slots," *2018 International Applied Computational Electromagnetics Society Symposium - China (ACES)*, 2018. DOI: 10.23919/ACCESS.2018.8669383
- [11] F. Gustrau., "RF and Microwave Engineering: Fundamentals of Wireless Communications," Wiley, 2012.
- [12] D. Deslandes and K. Wu, "Single-substrate integration technique of planar circuits and waveguide components," *IEEE Trans Microwave Theory Tech*, vol. 51, no. 2, p. 593–596, 2003. DOI: 10.1109/TMTT.2002.807820
- [13] D. M. Pozar, "Microwave Engineering", vol. 4, New York: John Wiley, 2012.
- [14] R. C. Caleffo, "Estudo e aplicações de guia de ondas integrados ao substrato em frequência de microondas," São Paulo, 2016.
- [15] D. Yoon, Y. Hong, Y. An, J. Jang, U. Pak and J. Yook, "High-gain planar tapered slot antenna for Ku-band applications," *IEEE Asia-Pacific Microwave Conference*, 2010.
- [16] R. Kazemi and A. Fathy, "Design of a wideband eight-way single ridge substrate integrated waveguide power divider," *IET Microwaves, Antennas & Propagation*, vol. 9, no. 7, p. 648–656, 2015. DOI: <https://doi.org/10.1049/iet-map.2014.0480>
- [17] C. C. R. Albuquerque, A. Gomes Neto, A. M. Oliveira, G. K. F. Serres and A. J. R. Serres, "Triple RSIW Fed Antipodal Vivaldi Antenna," *15th European Conference on Antennas and Propagation (EuCAP)*, 2021. DOI: 10.23919/EuCAP51087.2021.9411414
- [18] T. Djerafi and K. Wu, "Corrugated substrate integrated waveguide (siw) antipodal linearly tapered slot antenna array fed by quasi-triangular power divider," *Progress In Electromagnetics Research C.*, vol. 26, p. 139–151, 2011. DOI: 10.2528/PIERC11091912